

Weierstraß-Institut für Angewandte Analysis und Stochastik

im Forschungsverbund Berlin e.V.

Preprint

ISSN 0946 – 8633

Supercontinuum generation by the modulation instability

Ayhan Demircan¹, Uwe Bandelow¹

submitted: 31st October 2003

¹ Weierstrass Institute
for Applied Analysis and Stochastics
Mohrenstraße 39
10117 Berlin, Germany
E-Mail: demircan@wias-berlin.de
bandelow@wias-berlin.de

No. 881
Berlin 2003



2000 *Mathematics Subject Classification.* 35Q55, 35Q60, 78A60.

Key words and phrases. Nonlinear Schroedinger Equation, Optical Fiber, Four-Wave-Mixing.

Edited by
Weierstraß-Institut für Angewandte Analysis und Stochastik (WIAS)
Mohrenstraße 39
10117 Berlin
Germany

Fax: + 49 30 2044975
E-Mail: preprint@wias-berlin.de
World Wide Web: <http://www.wias-berlin.de/>

Abstract

We report on a numerical study of supercontinuum generation in a single-mode optical fiber by the modulation instability. An ultrabroadband octave-spanning continuum is generated for femtosecond pulses with subkilowatt peak power. In particular, we investigate the influence of higher-order effects such as third- and fourth-order dispersion, self-steepening and intrapulse Raman scattering on the supercontinuum generation.

1 Introduction

Supercontinuum (SC) generation in highly nonlinear optical fibers as microstructured fibers [1] or tapered fibers [2] has attracted considerable interest over the past few years [3]. The generation of broadband supercontinuum spectra can be achieved by various mechanisms. It has been shown, that the soliton decay due to third-order dispersion [4] or Raman scattering [5, 3] initiates the formation of the continuum in the anomalous dispersion regime. For the normal dispersion regime Coen *et al.* [6] attributed the primary mechanisms to the combined effect of stimulated Raman scattering and parametric four-wave-mixing, leading to a broad supercontinuum by using picosecond pulses with sub-kilowatt peak-power. Obviously, SC can be generated in both the anomalous and the normal dispersion regime but require different prerequisites to occur. We will pursue another possibility for the generation of extremely broad spectra, which is given by the modulation instability (MI) [7]. The latter can be interpreted as the result of four-wave-mixing (FWM) phase-matched by self-phase modulation and has usually to be taken into account in the anomalous dispersion regime. The impact of MI is especially enhanced in the vicinity of the zero-dispersion wavelength.

In this paper we present a numerical analysis of supercontinuum generation by the MI. This mechanism can initiate the formation of an ultrabroad continuum in both the normal and anomalous dispersion regime. In particular, the MI can still act in the normal dispersion regime if the fourth-order coefficient is negative. Furthermore, higher-order effects, as the third-order dispersion or the Raman-scattering are shown to be of less influence for the generation process, but can have a strong effect on the characteristics of the spectrum.

2 Model

To understand the mechanisms leading to the SC generation, we have solved numerically the one-dimensional generalized nonlinear Schrödinger equation (GNLSE) that describes the propagation of intense femtosecond pulses through a fiber. It is assumed that the pulse propagates along the z -axis within a retarded time frame $\tau = t - z/v_g$, moving at the group velocity v_g of the pulse. The general form of the GNLSE for the slowly varying complex envelope $A(z, \tau)$ of a pulse centered at frequency ω_0 is given by

$$\begin{aligned} \frac{\partial A}{\partial z} = & -\frac{i}{2}\beta_2\frac{\partial^2 A}{\partial\tau^2} + \frac{1}{6}\beta_3\frac{\partial^3 A}{\partial\tau^3} + \frac{i}{24}\beta_4\frac{\partial^4 A}{\partial\tau^4} - \frac{\alpha}{2}A \\ & + i\gamma|A|^2A - \frac{\gamma}{\omega_0}\frac{\partial(|A|^2A)}{\partial\tau} - i\gamma T_R A\frac{\partial|A|^2}{\partial\tau}. \end{aligned} \quad (1)$$

The linear terms on the right-hand side of Eq. (1) represent the group velocity dispersion (GVD), namely second-order (SOD), third-order (TOD) and fourth-order (FOD) dispersion and the attenuation term corresponding to the fiber loss α . The first nonlinear term represents self-phase modulation (SPM) with the nonlinear coefficient γ , which results from the intensity-dependent refractive index. The term proportional to γ/ω_0 results from the intensity dependence of the group velocity and causes self-steepening and shock formation at the pulse edge. The last term regards the intrapulse Raman scattering and originates from the delayed response, which causes a self-frequency shift, where T_R is related to the slope of the Raman gain. In our numerics we have used a standard de-aliased pseudospectral method with eighth-order Runge-Kutta integration scheme using adaptive stepsize control [8]. In the simulations described here, parameters are chosen close to the zero-dispersion wavelength ($\beta_2 \approx 0$) and the second dispersion zero ($\beta_3 \approx 0$), such that the dynamics is dominated by the action of the nonlinear terms. In particular, we consider propagation of an initially $\tau_0 = 600$ fs hyperbolic secant (sech) pulse, along a fiber with dispersion coefficients $\beta_2 = \pm 10^{-5}$ ps²/m, $\beta_3 = \pm 5 \times 10^{-7}$ ps³/m, $\beta_4 = \pm 2 \times 10^{-9}$ ps⁴/m and with nonlinear coefficient $\gamma = 0.1$ m⁻¹W⁻¹ and $T_R = 3$ fs. First we consider the anomalous dispersion regime, which leads to a high soliton order $N = 640$ for a peak power $P_0 = 64$ W, where $N^2 = \gamma P_0 \tau_0^2 / |\beta_2|$.

3 Continuum Generation

The output spectrum after a propagation distance of $L = 5$ m is depicted in Fig. 1, and shows an approximately symmetric spectrum, spanning an spectral width of about 7 THz. As in [9, 4] the supercontinuum exhibits a complicated structure with strong amplitude fluctuations. The pulse does not experience a notable asymmetric spectral broadening, which reflects the negligible role of higher-order effects in the chosen parameter region. To demonstrate this we perform calculations with the

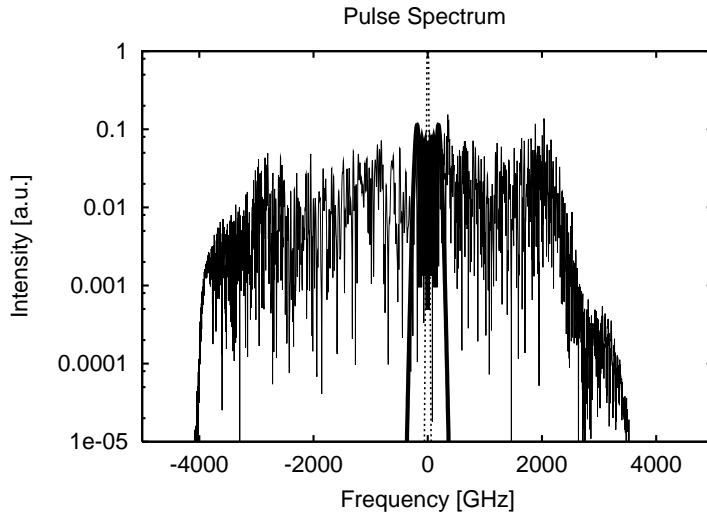


Figure 1: Spectra of an initially sech-pulse with $\tau_0 = 600$ fs with a peak input power $P_0 = 64$ W and $T_R = 3$ fs. Dotted: initial spectrum, solid: spectra after a distance of $L = 5$ m. Thin solid: GNLSE, thick solid: SPM only.

standard nonlinear Schrödinger equation (NLSE), where neither higher-order dispersive terms nor Raman scattering nor self-steepening contribution are included. The results are qualitatively the same as shown in Fig. 1, but the spectra are more symmetric and broader (not shown). The spectrum of the pulse broadened by self-phase modulation alone is drawn in Fig. 1 by the thick solid line, showing also a negligible role for the supercontinuum generation process. Hence the primary mechanism for the SC generation can be identified with the MI, in respect to which high-order solitons are unstable [10, 11]. Due to the absence of higher-order effects, their decay can only be initiated by numerical noise. The underlying MI acts directly from the beginning on the high-order soliton, where all other effects are still of less influence and leads to the generation of a Stokes and an anti-Stokes component. Fig. 2 (top) shows the appearance of two sidebands after $L = 0.2$ m (dotted line). The broadening and splitting of the central peak (between ± 200 GHz) are due to the self-phase modulation. The appearance of such spectral side lobes is the signature of the MI, which is accompanied by the emerge of secondary sidebands with further propagation. The phase-matched four-wave mixing procedure then explosively excites new frequencies and hence broadens and completes the spectrum. Therefore the SC shown in Fig. 1 turns out to be more than simply the amplification of noise. We note, that with higher peak powers the Stokes as well as the anti-Stokes components emerge at an earlier stage of the pulse propagation. In the time domain the modulation instability leads to small ripples at the center of the pulse, which build up over the entire pulse with further propagation along the fiber.

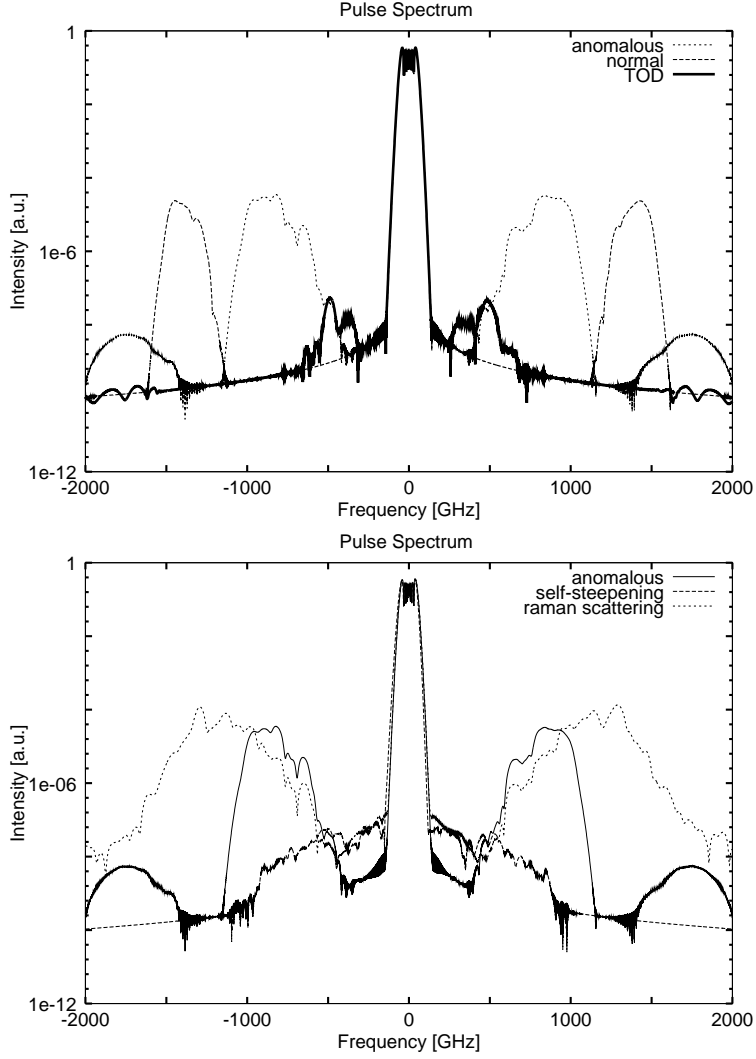


Figure 2: Spectra after a distance of $L = 0.2$ m when the higher-order effects influence the modulation instability. Top: higher-order dispersion: $\beta_2 = -1 \times 10^{-5} \text{ps}^2/\text{m}$, $\beta_3 = 0$, $\beta_4 = 0$ (dotted), $\beta_2 = -1 \times 10^{-5} \text{ps}^2/\text{m}$, $\beta_3 = -5 \times 10^{-7} \text{ps}^3/\text{m}$, $\beta_4 = 0$ (solid), $\beta_2 = 1 \times 10^{-5} \text{ps}^2/\text{m}$, $\beta_3 = 0$, $\beta_4 = -6 \times 10^{-9} \text{ps}^4/\text{m}$ (dashed). Bottom: higher-order nonlinearities: self-steepening (dashed), Raman-scattering ($T_R = 3$ fs) (dotted).

To investigate the influence of the higher-order effects on the SC generation, we included successively one of these effects separately. The results are shown in Fig. 2. As long as TOD is close to the second zero-dispersion no remarkable difference is observed, including the symmetry of the spectrum. An increased TOD ($\beta_3 = -5 \times 10^{-7} \text{ps}^3/\text{m}$, Fig. 2 (top), solid line) tends to suppress the MI, however. The formation of the spectral sidebands takes place for higher peak powers or for longer propagation distances. The corresponding Stokes and anti-Stokes frequencies emerge closer to the pump frequency, with a small asymmetry in intensity and position. With further propagation or increasing TOD the asymmetry between the sidebands is amplified. The sign of β_3 determines the asymmetry with respect to the red or the blue side of the spectrum. But this asymmetry in turn reduces the phase-match condition for the four-wave mixing, leading to a decelerated SC generation. The self-steepening effect has a similar impact. For low values of the self-steepening coefficient γ/ω_0 there is no influence on the MI and the continuum generation. With increasing self-steepening the spectrum becomes increasingly asymmetric. A strong impact of self-steepening readily suppresses the MI (see Fig. 2 (bottom), dashed line), such that the side lobes are diminished. The generation of a SC then disappears and the dynamics is determined by shock creation at the edge of the pulse.

The dashed line in Fig. 2 (top) displays the influence of the fourth-order dispersion (FOD). In the pure normal dispersion regime ($\beta_2 > 0, \beta_4 \geq 0$) the MI does not occur and, furthermore, noise perturbations are smoothed out. In the case of $\beta_4 < 0$ the modulation instability also occurs, especially in the vicinity of the zero-dispersion wavelength, such that this effect is also acting in the normal dispersion regime (Fig. 2 (top) dashed). The MI is further enhanced, when both coefficients β_2 and β_4 are negative. The spectral side bands are then shifted to higher frequencies, compared to the case with the contribution of β_2 alone. Therefore, in general, a negative β_4 leads to a complicated situation. In particular, the interplay between normal ($\beta_2 > 0$) and anomalous ($\beta_4 < 0$) dispersion can lead to unusual nonlinear effects.

The Raman scattering appears to have the most effective impact on the MI (Fig. 2, bottom, dashed). The MI is enhanced when the Raman term is added as a perturbation ($T_R = 3 \text{ fs}$). The spectral side bands emerge at a earlier stage of the propagation, with broader spectral widths and higher amplitudes. With further propagation an asymmetry between the Stokes and the anti-Stokes amplitude is imposed, where the Stokes amplitude is amplified and the anti-Stokes amplitude is absorbed. But the spectral broadening process suffers from the spectral asymmetry characteristics. The generated SC (Fig. 3), with an increased Raman gain ($T_R = 50 \text{ fs}$), shows its strong impact on the shape of the spectrum, but its negligible role on the spectral width.

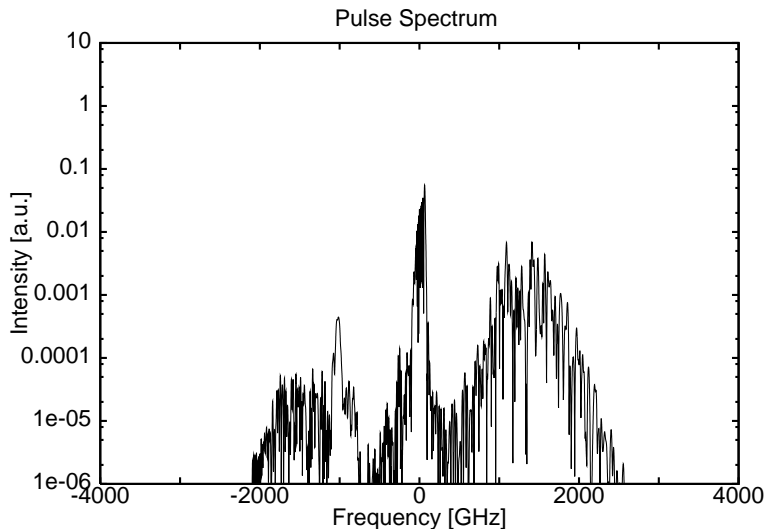


Figure 3: Spectrum of an initially sech-pulse with $\tau_0 = 600$ fs after a distance of $L = 0.5$ m for peak input power $P = 64$ W and $T_R = 50$ fs, where we drastically increased the Raman gain.

4 Conclusion

The overall observed behavior of SC generation is primarily determined by the MI for higher-order solitons. The onset of the MI is as earlier as higher the soliton order is. Because higher-order effects are not a prerequisite for the generation of SC, it is not restricted only to ultrashort sub-picosecond pulses, but appears for much longer pulses too. The MI enhances when higher-order dispersive terms are present. It can also appear in the normal dispersion regime $\beta_2 > 0$, if the fourth-order dispersion coefficient β_4 is negative. The characteristics of the spectrum, especially its shape, are determined by the action of the higher-order terms on the spectral side lobes. In particular the relative evolution of the Stokes and anti-Stokes components is affected by TOD and intrapulse Raman scattering.

References

- [1] J.K. Ranka, R.S. Windeler, and A.J. Stentz. Visible continuum generation in air-silica microstructure optical fibers with anomalous dispersion at 800 nm. *Opt. Lett.*, 2000.
- [2] T.A. Birks, W.J.Wadsworth, and P.St.J. Russel. Supercontinuum generation in tapered fibers. *Opt. Lett.*, 2000.
- [3] W.H. Reeves, D.V. Skryabin, F. Biancalana, J.C. Knight, P.St.J. Russel, F.G. Omenetto, A. Efimov, and A.J. Taylor. Transformation and control of ultrashort pulses in dispersion-engineered photonic crystal fibres. *Nature*, 2003.

- [4] J. Hermann, U. Griebner, N. Zhavoronkov, A. Husakou, D. Nickel, J.C. Knight, W.J. Wadsworth, P.St.J. Russel, and G. Korn. Experimental Evidence for Supercontinuum Generation by Fission of Higher-Order Solitons in Photonic Fibers. *Phys. Rev. Letters*, 2002.
- [5] G. Genty, M. Leptonen, H. Ludvigsen, J. Broeg, and M. Kaivola. Spectral broadening of femtosecond pulses into continuum radiation in microstructured fibers. *Opt. Express*, 2002.
- [6] S. Coen, A. Hing Lun Chau, R. Leonhardt, J.D. Harvey, J.C. Knight, W.J. Wadsworth, and P.St.J. Russel. Supercontinuum generation by stimulated raman scattering and parametric four-wave mixing in photonic crystal fibers. *J. Opt. Soc. Am. B*, 2002.
- [7] K.R. Tamura, H.K. Kubota, and M. Nakazawa. Fundamentals of Stable Continuum Generation at High Repetition Rates. *IEEE J. Quantum Electron.*, 2000.
- [8] U. Bandelow, A. Demircan, and M. Kesting. Simulation of Pulse Propagation in Nonlinear Optical Fibers. Technical report, WIAS, 2003.
- [9] A. L. Gaeta. Nonlinear propagation and continuum generation in microstructured optical fibers. *Optics Letters*, 27(11):924–926, June 2002.
- [10] M. Nakazawa, K. Suzuki, H. Kubota, and H. A. Haus. High-order solitons and the modulation instability. *Phys. Rev. A*, 1989.
- [11] M.J. Potasek and G.P. Agrawal. Self-amplitude-modulation of optical pulses in nonlinear dispersive fibers. *Phys. Rev. A*, 1987.